Journal of Colloid and Interface Science 466 (2016) 297–309

Contents lists available at ScienceDirect

Journal of Colloid and Interface Science

journal homepage: www.elsevier.com/locate/jcis

Application of a new bifunctionalized chitosan derivative with zwitterionic characteristics for the adsorption of Cu^{2+}, Co^{2+}, Ni^{2+}, and oxyanions of Cr^{6+} from aqueous solutions: Kinetic and equilibrium aspects

Francine Tatiane Rezende de Almeida [a], Bruno Christiano Silva Ferreira [c,d], Ana Luísa da Silva Lage Moreira [a], Rossimiriam Pereira de Freitas [c], Laurent Frédéric Gil [a,*], Leandro Vinícius Alves Gurgel [b,*]

[a] Group of Organic and Environmental Chemistry (GOEQ), Department of Chemistry, Institute of Biological and Exact Sciences, Federal University of Ouro Preto, Campus Universitário Morro do Cruzeiro, s/n°, Bauxita, 35400-000 Ouro Preto, Minas Gerais, Brazil
[b] Group of Physical Organic Chemistry (GPOC), Department of Chemistry, Institute of Biological and Exact Sciences, Federal University of Ouro Preto, Campus Universitário Morro do Cruzeiro, s/n°, Bauxita, 35400-000 Ouro Preto, Minas Gerais, Brazil
[c] Department of Chemistry, Institute of Exact Sciences (ICEX), Federal University of Minas Gerais, Avenida Antônio Carlos, 6627, Pampulha, 31270-901 Belo Horizonte, Minas Gerais, Brazil
[d] Departamento de Física e Química, Instituto de Ciências Exatas e Informática (ICEI), Pontifícia Universidade Católica de Minas Gerais, Av. Dom José Gaspar, 500, Coração Eucarístico, 30535-901 Belo Horizonte, Minas Gerais, Brazil

HIGHLIGHTS

- A new bifunctionalized chitosan (C2) with zwitterionic characteristics was prepared.
- Trimethylation of amine and esterification of hydroxyls with EDTAD was performed.
- C2 was used for the adsorption of Cu^{2+}, Co^{2+}, Ni^{2+}, and Cr^{6+} in aqueous solutions.
- Q_{max} of C2 for Cu^{2+}, Co^{2+}, Ni^{2+}, and Cr^{6+} were 0.698, 1.125, 0.725, and 1.91 mmol/g.
- Desorption (0.1 mol/L HNO_3) and reusability of the C2 adsorbent was also evaluated.

GRAPHICAL ABSTRACT

ARTICLE INFO

Article history:
Received 2 September 2015
Revised 22 November 2015
Accepted 20 December 2015
Available online 21 December 2015

Keywords:
Bifunctionalized chitosan
Adsorption
Copper

ABSTRACT

This study describes the synthesis of a new chitosan derivative (C2) with zwitterionic characteristics and its use for the removal of cationic species Cu^{2+}, Co^{2+}, and Ni^{2+} and anionic species of Cr^{6+} in a single aqueous solution. The new adsorbent was synthesized by quaternization of the amine group of chitosan and esterification of hydroxyl groups with EDTA dianhydride. These combined reactions gave both cationic and anionic characteristics to C2 with the release of quaternary ammonium groups and carboxylic groups. The capacity of C2 to adsorb Cu^{2+}, Co^{2+}, Ni^{2+}, and oxyanions of Cr^{6+} was evaluated in a batch process with different contact times, pH values, and initial concentrations. Adsorption isotherms were best fitted to the Langmuir and Sips models. The maximum adsorption capacities (Q_{max}) of C2 for adsorption of Cu^{2+}, Co^{2+}, Ni^{2+}, and Cr^{6+} were 0.698, 1.125, 0.725, and 1.910 mmol/g, respectively. The $\Delta_{ads}G°$ values

* Corresponding authors.
E-mail addresses: laurent@iceb.ufop.br (L.F. Gil), legurgel@iceb.ufop.br (L.V.A. Gurgel).

http://dx.doi.org/10.1016/j.jcis.2015.12.037

Cobalt
Nickel
Chromium
Desorption

were in the range from −20 to −28 kJ/mol. These values suggest a mixed mechanism controlling adsorption. Desorption studies using an aqueous solution consisting of 0.1 mol/L HNO_3 were carried out. The reusability of the recovered C2 adsorbent after desorption was also evaluated.

1. Introduction

Chitosan is a biopolymer obtained from the partial or complete deacetylation of chitin, which is a copolymer of *N*-acetyl-D-glucosamine and D-glucosamine units linked by β(1 → 4) glycosidic bonds, where *N*-acetyl-D-glucosamine units are predominant in the biopolymer chain [1,2]. Chitin is the second most renewable biopolymer available in nature after cellulose, with annual production estimated as 10^{10}–10^{11} tons [2]. It is vastly distributed in nature as a constituent of the exoskeleton of insects, carapaces of crustaceans such as crabs and shrimps [3], fungal cell walls, and algae components [4], which represent the most available raw materials for the industrial production of chitin and chitosan [3]. The isolation of chitin from raw materials consists of three basic steps: deproteinization, demineralization, and decolorization. Chitin is further deacetylated to obtain chitosan. Deacetylation can be performed by both chemical and enzymatic non-continuous batch methods. These methods are extensively used on an industrial scale for the production of chitosan and other derivatives [2]. Thus, chitin and chitosan are very advantageous natural resources when the economical recycling of wastes is considered [2].

The main advantage of chitosan compared to cellulose with respect to the preparation of new derivatives is the presence of a primary amine group at the C-2 position of the pyranosidic ring. This amine group allows the preparation of various new materials with novel chemical properties using different synthesis strategies for new applications [1]. One of these applications is as an adsorbent material for the removal of heavy metal ions and dyes in cationic and/or anionic forms from water and wastewater. However, chitosan is known to be very sensitive to changes in pH as it can either form a gel or dissolve [1]. Therefore, the chemical modifications of chitosan should always take into account the improvement of its properties such as solubility and swelling without decreasing its performance as an adsorbent material for the removal of various pollutants [1].

The production of chitosan derivatives for the treatment of water and wastewater containing metal ions has been extensively investigated by various researchers in recent years [1,5,6,7,8,9,10]. The chemical modifications of chitosan include the grafting of organic ligands containing carboxylic acid, iminoacetic and iminodiacetic, phosphate, thiol, and quaternary ammonium groups among others capable to form complexes with metallic cations such as Cu^{2+}, Cd^{2+}, Co^{2+}, Cr^{3+}, Cr^{6+}, Hg^{2+}, Ni^{2+}, Pb^{2+}, and Zn^{2+} [6,8] or interact electrostatically with oxyanions such as $HAsO_4^{2-}$, AsO_2^- [11], CrO_4^{2-}, and $Cr_2O_7^{2-}$ [12]. Among the numerous chitosan derivatives synthesized for the removal of heavy metals is uncommon to find adsorbent materials with zwitterionic characteristics that have affinity for both cationic and anionic species [13].

The management of hazardous wastes containing heavy metals is of major public concern. The increasing levels of toxic heavy metals in the form of metallic cations and/or oxyanions discharged into the environment have also attracted substantial attention due to the adverse effects on receiving water bodies and living organisms [14]. The increasing levels of heavy metals are also a consequence of the fast expansion of industrial products such as batteries, electronics, fertilizers, fungicides, metal plating, metals, mining, paints, paper, pesticides, petrochemicals, pigments, tanneries, textiles, and preserved wood products [12,15,16]. Although some heavy metals such as Co^{2+}, Cu^{2+}, Ni^{2+}, and Zn^{2+}, among others, are essential to human life and health, they become detrimental when taken in excess [15,17]. In addition, heavy metals are non-biodegradable and are known to biomagnify and bioaccumulate through the food chain, causing adverse effects to living organisms [15,17]. The adverse effects caused by the intake of excess of heavy metals have been well documented by Klaassen [18].

Various treatment methods such as adsorption, chemical precipitation, electrodialysis, electrochemical, ion exchange, reverse osmosis, precipitation, and ultra- and nanofiltration have been established for the isolation, recovery, and/or elimination of metal ions from water and industrial wastewater [15,17,19]. However, the method to be employed depends on the nature of the heavy metal ions, concentration, pH, the amount of effluent to be treated, treatment performance, investment costs, energy requirements, available area, legislation (quality of the treated effluent), and the production of toxic sludge, among other factors [19]. Adsorption has emerged as one of the more promising alternative treatments in recent years [19]. Some advantages of adsorption are its performance, ease of operation, the possible use of renewable and biodegradable adsorbents, low energy requirements, capacity to treat very dilute wastewater, recovery and recycling of the adsorbent, and recovery of heavy metals [19].

This study aimed to produce a new bifunctionalized adsorbent material from chitosan to remove Co^{2+}, Cu^{2+}, Ni^{2+}, and oxyanions of Cr^{6+} from single aqueous solution and thereby to produce a versatile adsorbent. This new adsorbent was synthesized by quaternization of amine group of chitosan followed by esterification of hydroxyl groups with EDTA dianhydride (EDTAD). This synthesis strategy provided both cationic and anionic characteristics to the modified chitosan with the release of quaternary ammonium groups and carboxylic acid functions. The adsorption studies were assessed as a function of the contact time (kinetics), solution pH, and initial metal ion concentration.

2. Experimental

2.1. Materials

The starting material was medium molecular weight chitosan (cat. no. 448877; 75–85% deacetylated) and molecular sieve (cat. no. 69839 Fluka), which were purchased from Sigma–Aldrich. *N*, *N*-dimethylformamide (DMF), pyridine, methyl iodide, NaH_2PO_4, and Na_2HPO_4 were purchased from Vetec (Brazil). EDTA (disodium salt) and acetic anhydride were purchased from Synth (Brazil) and used without further purification. Acetone, diethyl ether, ethanol, NaOH, HCl, $ClCH_2COOH$, CH_3COOH, CH_3COONa, $Na_2Cr_2O_7$, $NaHCO_3$, $CuSO_4.5H_2O$, $CoCl_2.6H_2O$, $NiCl_2.6H_2O$ were purchased from Synth (Brazil). Quantitative filter paper (black ribbon, JP 41, cat. no. 3509-1, 12.5 diameter, ash content of 0.00009 g, and grammage of 80 g/cm^2) was purchased from JProlab (Brazil). All metal ion solutions were prepared in deionized water (Millipore, model Milli-Q®). The molecular sieve 3 Å was previously activated in an oven at 150 °C for 2 h before use. DMF was stored with molecular sieves before use. Pyridine was refluxed in a round-bottomed flask with NaOH pellets for 12 h and distilled before use.

2.2. Quaternization of amine groups of chitosan

Chitosan (C) (40.0 g; MW = 171.45 g/mol based on degree of deacetylation) was transferred to a 2 L round-bottom flask and 800 mL of DMF and 800 mL of aqueous NaOH solution (0.28 mol/L) were added. Then, the flask was placed in an ice-water bath at 0 °C for 20 min. After cooling the flask, 30 mL (0.482 mol) of CH_3I were slowly added and the suspension was magnetically stirred at 25 °C for 48 h (Corning®, model PC-420D). The molar ratio of 1:0.96:2.07 for C:NaOH:CH_3I was adopted to avoid *O*-alkylation of hydroxyl groups at the positions C-3 and C-6 of C [20]. The swollen quaternized chitosan (C1) was poured into a 5 L Becker containing ice-cooled acetone (4 L) under soft magnetic stirring for precipitation. Then, C1 was separated by vacuum filtration using sintered glass Büchner funnel (porosity 3) and washed with acetone. The alkylation reaction was performed twice to increase the amount of trialkylated amines in C1. Finally, C1 was dried at 60 °C and stored in a desiccator for subsequent acylation with EDTA dianhydride (EDTAD). The percent weight gain (*pwg*) and amount of ammonium groups ($n_{N^+(CH_3)_3}$) were determined as described in Sections 2.4.1 and 2.4.2.

2.3. Acylation of quaternized chitosan (C1) with EDTAD

The EDTA dianhydride (EDTAD) was prepared using the method described by Karnitz et al. [21]. C1 (12.63 g) was transferred to a round-bottom flask and 37.9 g of EDTAD (EDTAD-to-C1 ratio = 3:1) and 530 mL of anhydrous DMF (DMF-to-C1 ratio of 42) and 75 g anhydrous calcium chloride were added. The flask was equipped with a reflux condenser attached to a drying tube packed with anhydrous calcium chloride. Then, the flask was placed in an oil bath at 75 °C and magnetically stirred for 24 h (Corning®, model PC-420D). At the end of the reaction time, the suspension was separated by vacuum filtration in a sintered glass Büchner funnel (porosity 3) and washed with DMF, deionized water, saturated solution of sodium bicarbonate, deionized water, ethanol, and acetone. Then, the bifunctionalized chitosan (C2) was dried in an oven at 80 °C for 1 h and left to cool in a desiccator. The *pwg* was determined as described in Section 2.4.1.

2.4. Characterization of the chitosan derivatives

2.4.1. Percent weight gain

The percent weight gain (*pwg*) for the chemical modifications of C to produce C1 and C2 was calculated using Eq. (1).

$$pwg/(\%) = \left(\frac{m_f - m_i}{m_i}\right) \times 100 \quad (1)$$

where m_f and m_i (g) are the weights of the chitosans after and before chemical modification, respectively.

2.4.2. Determination of the amount of quaternary ammonium groups ($n_{N^+(CH_3)_3}$) of C1

The amount of quaternary ammonium groups ($n_{N^+(CH_3)_3}$) of C1 was determined by conductimetric titration using the method described by Spinelli et al. [12]. A sample of C1 (200.0 mg) was suspended in a 250 mL Becker containing 200 mL of deionized water and an aqueous 0.1 mol/L $AgNO_3$ solution was added drop-by-drop to form a precipitate of AgI. This test was performed in triplicate. The amount of quaternary ammonium groups was determined using Eq. (2) as follows:

$$n_{N^+(CH_3)_3}/(\text{mmol/g}) = \frac{C_{AgNO_3} V_{AgNO_3}}{w_{C1}} \quad (2)$$

where C_{AgNO3} (mmol/L) is the concentration of aqueous $AgNO_3$ solution, V_{AgNO3} (L) is the volume of aqueous $AgNO_3$ solution expended titrating the amount of iodine ions present in C1, and w_{C1} (g) is the weight of C1.

2.4.3. Fourier transform infrared spectroscopy (FTIR) analysis

Samples for analyses were prepared mixing 1 mg of dried powder of C, C1, or C2 with 100 mg of spectroscopy grade KBr and pressed to obtain 13 mm diameter KBr pellets. The FTIR spectra were recorded on FTIR spectrometer (Shimadzu, model IR-408) with the detector set at a resolution of 4 cm^{-1} from 500 to 4000 cm^{-1} and 32 scans per sample.

The degree of acetylation (*DA*) of C was determined by FTIR using Eq. (3) as follows [22]:

$$DA = \frac{(A_{1320}/A_{1420} - 0.3822)}{0.03133} \quad (3)$$

where A_{1320}/A_{1420} is the absorbance ratio at 1320 and 1420 cm^{-1}, respectively.

2.4.4. Elemental analysis

Samples of C, C1, and C2 were previously washed with diethyl ether in a sintered Büchner glass funnel (porosity 3), and dried at 25 °C in a desiccator under vacuum for 5 h. Samples were analyzed on a CHN Perkin Elmer Series II equipment. The analyses were performed in duplicate for each sample.

2.4.5. Solid state ^{13}C NMR analysis

The solid-state ^{13}C NMR spectra of C and C2 were obtained on a Bruker DRX-400 spectrometer at the frequency of 400 MHz. The acquisition time was 0.034 s. Each spectrum was obtained with an accumulation of 5000 scans.

2.4.6. Point of zero charge (PZC)

The point of zero charge (PZC) for C2 was determined using the mass titration method as described by Noh and Schwarz [23]. Three aqueous 0.01 mol/L $NaNO_3$ solutions with pH values of 3, 6, and 9 were prepared by adjusting the pH of the solutions using aqueous 0.1 mol/L HNO_3 and 0.1 mol/L NaOH solutions. Four aliquots of 10.0 mL were taken from the solutions of different pH and transferred to 50 mL Erlenmeyer flasks. Different amounts of C2 were then added to the Erlenmeyer flasks to give suspensions of 5%, 10%, 30%, and 60% (w/w). The equilibrium pH values were measured after 24 h of shaking at 25 °C and 130 rpm using a pH meter (Hanna Instruments, model HI 223) to obtain the PCZ.

2.5. Adsorption experiments

2.5.1. Effect of the solution pH on metal ion uptake by C2

Adsorption experiments for each metal ion were performed to determine the effect of the solution pH on metal ion adsorption on C2. Samples of 20.0 mg of C2 were weighed into 250 mL Erlenmeyer flasks and 100.0 mL of buffered metal ion solution in each pH were added (100 mg/L for Cu^{2+}, 70 mg/L for Co^{2+} and Ni^{2+}, and 25 mg/L for Cr^{6+}). The flasks were incubated at 25 °C in a shaking incubator (Tecnal, model TE-424) and stirred at 150 rpm for 6 h for Cu^{2+}, Co^{2+}, and Ni^{2+} and 12 h for Cr^{6+}. These time periods were enough to attain equilibrium. The pH range studied for adsorption was from 2.0 to 5.5 for Cu^{2+}, from 3.0 to 6.0 for Co^{2+}, from 2.0 to 7.5 for Ni^{2+}, and from 2.0 to 7.5 for Cr^{6+}. The buffer solutions used were 0.1 mol/L $ClCH_2COOH/ClCH_2COONa$ (from pH 2.0 to 3.5), 0.1 mol/L CH_3COOH/CH_3COONa (from pH 3.75 to 5.5), and 0.1 mol/L NaH_2PO_4/NaH_2PO_4 (from pH 6.0 to 9.0). These buffer solutions and pH values were chosen considering the solubility of metal ions in each buffer solution. The maximum pH values of each metal ion solution to avoid the formation of hydrolyzed species and

precipitation was calculated using the concentration of each metal ion solution and solubility product constant (K_{sp}) for $Co(OH)_2$ (5.92×10^{-15}), $Cu(OH)_2$ (1.8×10^{-20}), and $Ni(OH)_2$ (5.48×10^{-16}) [24]. The adsorption experiments were performed in duplicate. After the equilibrium was reached, the suspensions were filtered off by single filtration (JP-41 filter paper) and the concentration of metal ions was determined by flame atomic absorption spectroscopy (FAAS) (Hitachi, model Z-8200) (λ_{Co} = 240.7 mm, λ_{Cu} = 324.8 mm, λ_{Ni} = 232 mm, and λ_{Cr} = 357.9 mm). The amount of each metal ion adsorbed on C2 at equilibrium was calculated using Eq. (4) as follows:

$$q_e/(\text{mg/g}) = \frac{(C_i - C_e)V}{w_{C2}} \quad (4)$$

where C_i and C_e (mg/L) are the initial and equilibrium metal ion concentrations, V (L) is the volume of metal ion solution, and w_{C2} (g) is the weight of C2.

2.5.2. Effect of contact time (kinetics) on metal ion uptake by C2

The uptake of Co^{2+} Cu^{2+}, Ni^{2+}, and Cr^{6+} by C2 was studied as a function of time in order to determine the adsorption kinetics. Samples of 20.0 mg of C2 weighed into cylindrical glasses (1.8 mm height × 2.2 mm diameter) were added to 250 mL Erlenmeyer with 100.0 mL of buffered metal ion solution (70 mg/L and pH 4.5 for Cu^{2+}, 20 mg/L and pH 4.5 for Co^{2+} and pH 7.5 for Ni^{2+}, and 25 mg/L and pH 2.0 for Cr^{6+}) previously thermostated at 25 °C in a shaking incubator for 1 h (Tecnal, model TE-424, Piracicaba, SP, Brazil). The buffer solutions used for each pH level were those described in Section 2.5.1. The flasks were shaken under constant stirring at 150 rpm for different time intervals. After each period of time, the suspensions were filtered off by single filtration (JP-41 filter paper) and the concentration of metal ions was determined by FAAS, as described in Section 2.5.1. The adsorption experiments were made in duplicate. The amount of each metal adsorbed on C2 in each period of time was calculated using Eq. (5) as follows:

$$q_t/(\text{mg/g}) = \frac{(C_i - C_t)V}{w_{C2}} \quad (5)$$

where q_t (mg/g) is the amount of metal ion adsorbed on C2 at a time t, V (L) is the volume of metal ion solution, C_i and C_t (mg/L) are the metal ion concentrations at 0 and time t, and w_{C2} (g) is the weight of C2.

2.5.3. Effect of initial metal ion concentration on metal ions uptake by C2 (adsorption isotherms)

The effect of initial metal ion concentration on metal ion uptake by C2 was performed by varying the initial concentration of metal ion solutions in order to obtain adsorption isotherms. Samples of 20.0 mg of C2 were weighed into 250 mL Erlenmeyer flasks and 100.0 mL of buffered metal ion solutions with concentrations varying from 4.2 to 70 mg/L for Co^{2+}, from 28 to 42 mg/L for Cu^{2+}, from 10.5 to 33.6 mg/L for Ni^{2+}, and from 22 to 100 mg/L for Cr^{6+} were added to each flask. Adsorption equilibrium times and pH values were those of higher equilibrium adsorption capacity determined by adsorption experiments as a function of solution pH (Section 2.5.1) (pH 4.5 for Co^{2+} and Cu^{2+}, 7.5 for Ni^{2+}, and 2.0 for Cr^{6+}) and time (Section 2.5.2) (360 min for Co^{2+}, Cu^{2+}, and Ni^{2+} and 720 min for Cr^{6+}). The flasks were thermostated at 25 °C in a shaking incubator (Tecnal, model TE-424, Piracicaba, SP, Brazil) for the required time to reach equilibrium. After equilibrium was reached, the suspensions were filtered off by single filtration (JP-41 filter paper) and the concentration of metal ions was determined by FAAS, as described in Section 2.5.1. The equilibrium adsorption capacity was calculated using Eq. (4).

2.6. Desorption

Three samples of 20.0 mg of C2 were loaded with 100.0 mL of buffered metal ion solution with the same metal ion concentrations, pH values, and equilibrium adsorption times (360 min for Co^{2+}, Cu^{2+}, and Ni^{2+} and 720 min for Cr^{6+}) previously described in Section 2.5.2. Samples of C2 loaded with each metal ion were filtered off by a single filtration, rinsed with an excess of deionized water in order to remove metal ions not adsorbed on C2, and dried at 60 °C for 12 h. Two samples of 20.0 mg of C2 loaded with each metal ion were weighed into 250 mL Erlenmeyer flasks and 100.0 mL of aqueous 0.1 mol/L HNO_3 solution was added. The flasks were placed in a thermostated shaker incubator (Tecnal, model TE-424, Piracicaba, SP, Brazil) at 25 °C and 130 rpm for 7 h. Further procedures for separation of the solid and liquid fractions and determination of metal ion concentration were those as earlier described in Section 2.5.1. The desorption efficiency (E_{des}) was calculated using Eq. (6) as follows:

$$E_{des}/\% = \left(\frac{C_e\, V}{Q_{T,max} w'_{C2}}\right) \times 100 \quad (6)$$

where E_{des} (%) is the desorption efficiency, C_e (mg/L) is the equilibrium metal ion (M^{n+}) concentration in aqueous desorption solution, V (L) is the volume of desorption solution, $Q_{T,max}$ (mg/g) is the maximum adsorption capacity determined by loading metal ions on the C2 before the desorption study, and w'_{C2} (g) is the weight of the C2 adsorbent contained in $w_{C2,M^{n+}}$, which was the weight of the material (C2 adsorbent loaded with M^{n+}) used in the desorption study.

The weight of the C2 adsorbent contained in $w_{C2,M^{n+}}$ is calculated using Eq. (7) as follows:

$$w'_{C2}/g = \frac{w_{C2,M^{n+}} w_{C2}}{\left(\frac{Q_{T,max} w_{C2}}{1000}\right) + w_{C2}} \quad (7)$$

Rearranging and simplifying Eq. (7) yields Eq. (8) as follows:

$$w'_{C2}/g = \frac{w_{C2,M^{n+}}}{\left(\frac{Q_{T,max}}{1000}\right) + 1} \quad (8)$$

where $w_{C2,M^{n+}}$ (g) is the weight of the C2 adsorbent loaded with metal ions.

2.6.1. Reuse of the C2 adsorbent

Samples of 20.0 mg of C2 (dried in an oven at 60 °C for 12 h) obtained from each desorption study with different metal ions were weighed into 250 mL Erlenmeyer flasks and 100.0 mL of buffered metal ion solution with the same metal ion concentration and pH was added as previously described in Section 2.5.2. The flasks were transferred to a thermostated shaker incubator at 25 °C and 130 rpm and kept for the same time for each metal ion as described in Section 2.6. Further experimental procedures were the same adopted as described in Section 2.5.1. The re-adsorption efficiency (RE) of the C2 adsorbent for a new cycle of adsorption was calculated using Eq. (9) as follows:

$$RE/\% = \frac{Q_{RE,max}}{Q_{T,max}} \times 100 \quad (9)$$

where RE (%) is the re-adsorption efficiency and $Q_{RE,max}$ (mg/g) is the maximum adsorption capacity redetermined in the re-adsorption study.

The value of $Q_{RE,max}$ is calculated using Eq. (10) as follows:

$$Q_{RE,max}/(\text{mg/g}) = \frac{w'_{M^{n+}} + w''_{M^{n+}}}{w_{C2}} \quad (10)$$

where $w'_{M^{n+}}$ (mg) is the weight of metal ions not desorbed from the C2 adsorbent after the desorption study and $w''_{M^{n+}}$ (mg) is the weight

of metal ions adsorbed on the C2 adsorbent in the re-adsorption study.

The values of $w'_{M^{n+}}$ and $w''_{M^{n+}}$ are calculated using Eqs. (11) and (12) as follows:

$$w'_{M^{n+}} = \left[\left(w_{C2,M^{n+}} - w'_{C2}\right)\left(1 - E_{des}/100\right)\right] \times 1000 \quad (11)$$

$$w''_{M^{n+}} = \left(C_i - C_e\right)V \quad (12)$$

3. Results and discussion

3.1. Synthesis and characterization of C2

The synthetic route used to produce C2 is presented in Fig. 1. In the first step of the synthesis strategy, the medium molecular weight chitosan (C) was treated twice with methyl iodide and NaOH in DMF/H_2O (1:1, v/v) at 25 °C for 48 h to obtain *N*,*N*,*N*-trimethyl chitosan (C1), an adsorbent containing positively charged quaternary ammonium groups capable of adsorbing oxyanions through ion exchange. This synthesis condition was used by Rúnarsson et al. [20] to favor significant amounts of *N*,*N*,*N*-trimethylation to the detriment of *N*-monomethylation and *O*-methylation. In the second step of the synthetic strategy the C1 was esterified with EDTA dianhydride (EDTAD) in DMF at 75 °C for 24 h to produce bifunctionalized chitosan (C2) containing carboxylic acid and amine groups capable of adsorbing metal ions in cationic form through ion exchange and complexation.

The degree of acetylation (*DA*) in the starting chitosan was found to be 24.3% (Section 2.4.3). After the quaternization reaction of the amine groups, the amount of quaternary ammonium groups ($n_{N^+(CH_3)_3}$) was found to be 0.494 mmol/g (Section 2.4.2), which corresponds to a *N*,*N*,*N*-trimethylation degree of 28%. The *pwg* after methylation reaction of chitosan was 85.5% (Section 2.4.1). It was not possible to estimate the number of carboxylic acid groups introduced after esterification of C1 with EDTA dianhydride due to the low pK_a values of the EDTA moiety grafted onto C2. The *pwg* after the esterification reaction of C1 with EDTAD was 41.8%.

The characterization of C, C1, and C2 was performed by elemental analysis of carbon (C), hydrogen (H), and nitrogen (N) as presented in Table 1. The data of elemental analysis of C, H, and N of C, C1, and C2 showed that the successive chemical modifications of C to produce C2 decreased the nitrogen and hydrogen contents with an increase in the carbon content. These results are in concordance with the introduction of methyl groups to produce C1, which increased the carbon content. The introduction of EDTAD on C1 to obtain C2 exhibited the same tendency, as EDTAD has more atoms of carbon (10) than nitrogen (2).

Characterization of C1 and C2 was also accomplished by FTIR spectroscopy. FTIR spectra of C and C1 are shown in Fig. 2a and b. Quaternization reaction of C was demonstrated by the analysis of the FTIR spectrum of C1 (Fig. 2a) in the region between 1200 and 1700 cm^{-1}. The main evidences of quaternization of chitosan are: (1) the appearance of the band at 1475 cm^{-1}, which is attributed to the asymmetric angular deformation of C—H bonds of methyl groups [25]. This signal is absent in the FTIR spectrum of C. (2) The band at 1577 and 1559 cm^{-1}

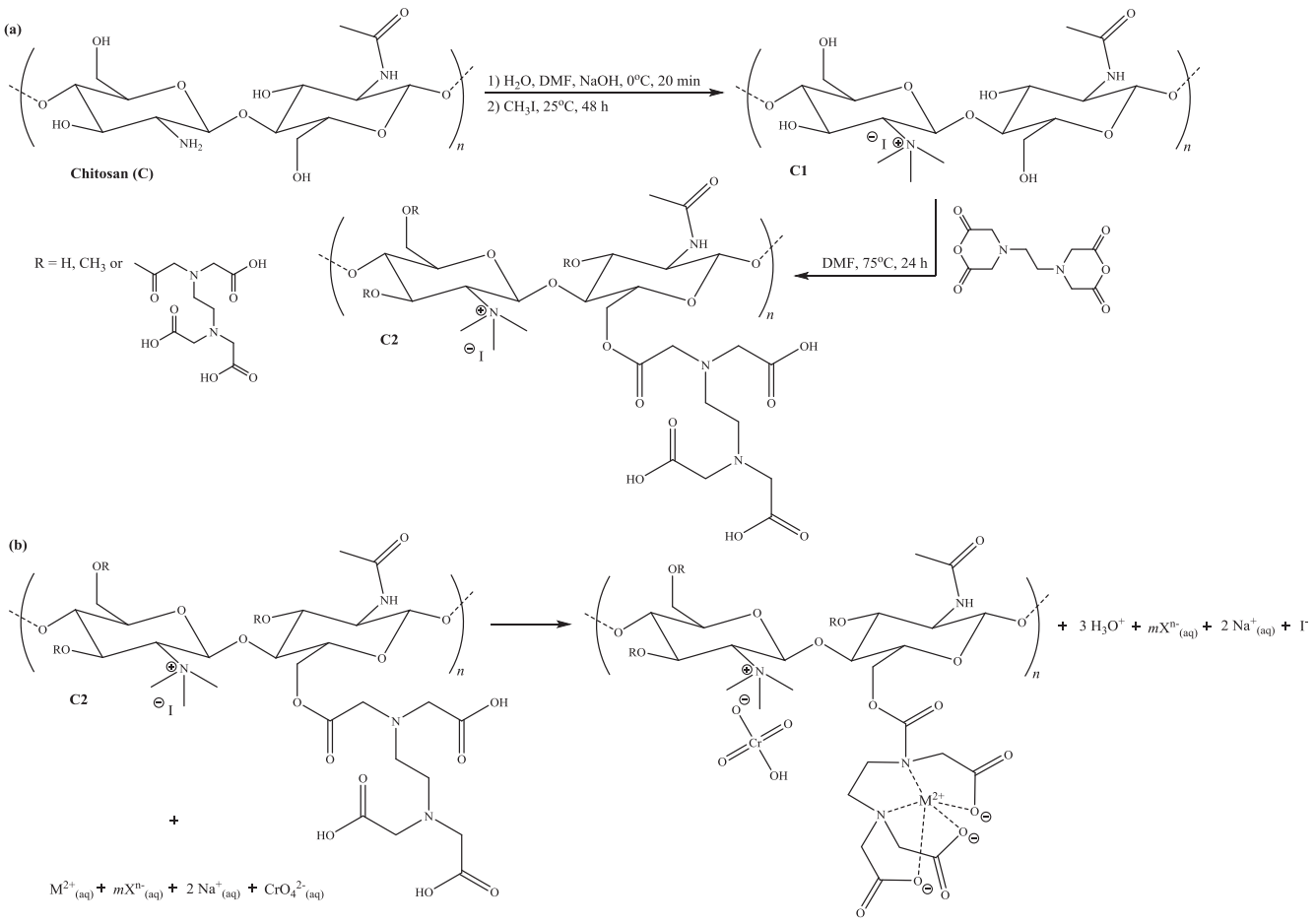

Fig. 1. (a) Synthetic route used to prepare C2 adsorbent and (b) the suggested mechanism for the adsorption of metal ions in cationic and anionic forms.

Table 1
Results of elemental analysis for C, C1, and C2.

Material	C (%)	H (%)	N (%)
C	38.82	7.00	6.63
C1	41.34	6.87	5.19
C2	45.49	5.65	3.05

related to the angular deformation of N—H bond of amine group, which occurred in both spectra of C and C1; however, these bands were weakened in the spectrum of C1 due to partial methylation of the amine group. (3) The appearance of bands at 1415–1430 cm^{-1}, which were assigned to the characteristic absorption of N—CH_3 [25].

FTIR spectra of C1 and C2 are shown in Fig. 2b. The comparison between the spectra of C2 and C1 revealed the appearance of a strong band at 1748 cm^{-1}, which can be attributed to axial deformation of the ester bond (—O—C=O) and bands at 1578 and 1422 cm^{-1}, which were attributed to asymmetric and symmetric axial deformations of carbonyl groups (C=O) of carboxylate ions (—COO^-Na^+). The appearance of these new bands related to the introduction of new carbonyl groups in C2 indicates that the esterification of the hydroxyl groups of C1 with EDTAD was accomplished.

FTIR spectra of C2 (unloaded with metal ions) and C2 after desorption of Co^{2+}, Cu^{2+}, Ni^{2+}, and Cr^{6+} are shown in Fig. 2c. The same infrared bands attributed for C2, which proved the success of chemical modification of C with methyl iodide and EDTAD were confirmed in the FTIR spectra of the adsorbents after desorption with an aqueous 0.1 mol/L HNO_3 solution. This means that there was no ester bond hydrolysis during the desorption process, which could be confirmed by presence of ester band at 1748 cm^{-1} as highlighted in Fig. 2c.

C and C2 were also characterized by solid-state ^{13}C NMR spectroscopy. The SS ^{13}C NMR spectra of C and C2 are shown in Fig. 3a and b. In Fig. 3a, the signals at 57.3, 60.9, and 81.8 ppm correspond to the carbon atoms at C-2, C-6 and C-4 of pyranosidic ring. The signal at 75.9 ppm can be attributed to C-3 and C-5 with the superposition of signals. The signals at 105.4 and 22.5 ppm can be attributed to C-1 and the methyl of the acetamide group [26], respectively. Quaternization of the amine group at C-2 and esterification of hydroxyl groups at C-3 and C-6 with EDTAD were demonstrated through the analysis of SS ^{13}C NMR spectra of C2 (Fig. 3b). The main evidences of C2 formation are the appearance of signals at 30, 50, and 170–175 ppm, which can be attributed to the methyl groups of quaternary ammonium [27], methylene groups between the tertiary amines of the EDTA moiety [28], and the carbon of the carbonyl groups of the ester and carboxylic acid in the EDTA moiety, respectively.

The experimental mass titration curves (figure not shown) for the evaluation of point of zero charge (PZC) for C2 converged to PZC value of 4.8. Therefore, pH values higher than 4.8 should ensure a predominantly negatively charged surface for C2, promoting the adsorption of cationic species, while pH values below 4.8 should ensure a predominantly positively charged surface for C2, promoting the adsorption of anionic species.

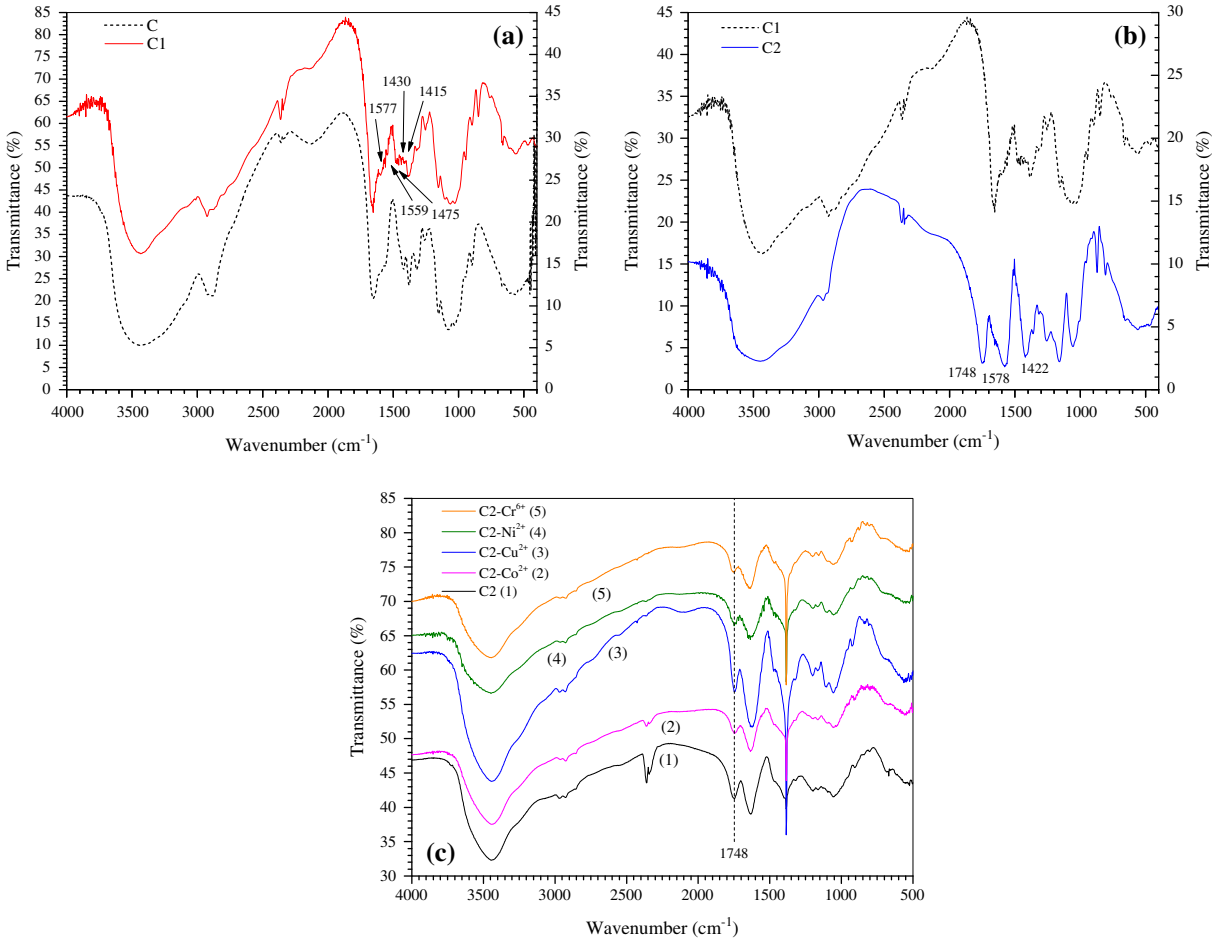

Fig. 2. FTIR spectra of (a) C and C1, (b) C1 and C2, and (c) C2 and C2 after desorption of Co^{2+}, Cu^{2+}, Ni^{2+}, and Cr^{6+} (the spectra of C2 and C2 after desorption (c) were vertically shifted by −15%, −15%, +5%, +5%, and +10%).

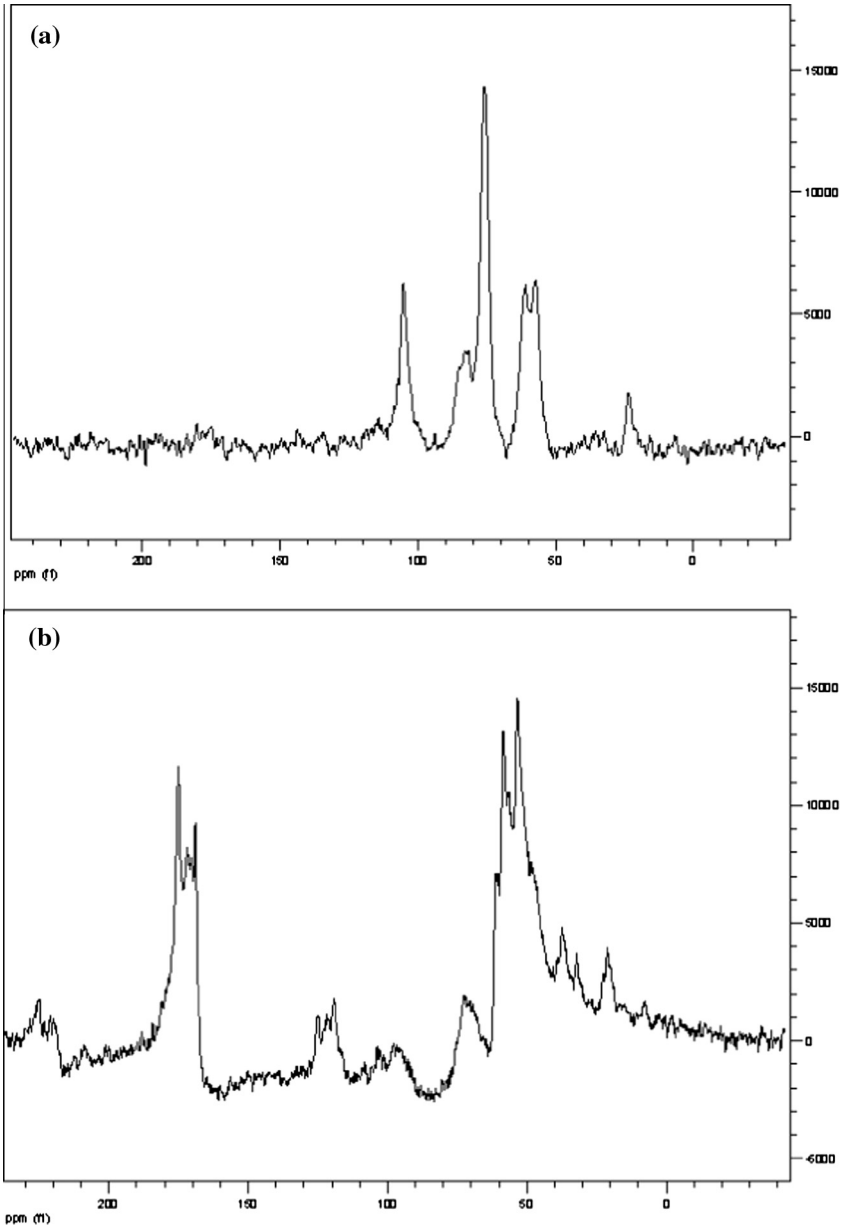

Fig. 3. Solid-state ^{13}C NMR spectra of (a) C and (b) C2.

3.2. Adsorption study of metallic cations Co^{2+}, Cu^{2+}, and Ni^{2+} and oxyanions of Cr^{6+} on C2 in single aqueous solutions

The studies of the adsorption properties of the C2 adsorbent were performed for each metallic cation and anions in single component aqueous solutions. The adsorption capacity of C2 was evaluated as a function of contact time (kinetics), the pH of the solution, and the initial concentration of each metallic cation and anion.

3.2.1. Adsorption kinetics

Adsorption kinetics is one of the most important parameters for the rational design of a wastewater treatment plant for the removal of different pollutants [29]. Experiments to investigate the effect of contact time on the adsorption of Co^{2+}, Cu^{2+}, Ni^{2+}, and Cr^{6+} on the C2 adsorbent were carried out to determine the adsorption equilibrium time. The effect of contact time on the adsorption of each metallic cation and oxyanions of Cr^{6+} on C2 was carried out using buffered adsorbate solutions of known concentrations (70 mg/L for Cu^{2+}, 20 mg/L for Co^{2+} and Ni^{2+}, and 25 mg/L for Cr^{6+}) at pH values of 4.5 for Co^{2+} and Cu^{2+}, 7.5 for Ni^{2+}, and 2.0 for Cr^{6+} at 25 °C, 150 rpm, and an adsorbent dose of 0.2 g/L.

The pseudo-first-order kinetic model of Lagergren [30] assumes that the adsorption rate is a function of the adsorption capacity as shown in Eq. (13):

$$\frac{dq_t}{dt} = k_1(q_e - q_t) \tag{13}$$

where q_e and q_t (mg/g) are the adsorption capacities at equilibrium t_e and time t (min) and k_1 (min^{-1}) is the pseudo-first-order rate constant. Rearranging and integrating Eq. (13) for the boundary conditions of $q_t = 0$ at $t = 0$ and $q_t = q_t$ at $t = t$ yields Eq. (14) as follows:

$$q_t = q_e(1 - \exp^{-k_1 t}) \tag{14}$$

The pseudo-second-order kinetic model of Ho and McKay [31] also assumes that the adsorption rate is a function of adsorption capacity; however, it states that the rate-limiting step may be

controlled by chemical adsorption involving valency forces through sharing or exchange electrons between the adsorbent and the adsorbate as follows in Eq. (15):

$$\frac{dq_t}{dt} = k_2(q_e - q_t)^2 \quad (15)$$

where k_2 (g/mg min) is the pseudo-second-order rate constant. Rearranging and integrating Eq. (15) for the boundary conditions of $q_t = 0$ at $t = 0$ and $q_t = q_t$ at $t = t$ yields Eq. (16) as follows:

$$q_t = \frac{k_2 q_e^2 t}{1 + k_2 q_e t} \quad (16)$$

The experimental kinetic data (see Supplementary Table 1) were modeled by non-linear regression (NLR) using Microcal OriginPro® 2015 software and the pseudo-first- and second-order kinetic models. The software was set to use the Levenberg–Marquardt algorithm and the weight method named statistical [Eq. (17)]. In the latter, the weights are used to minimize the chi-square (χ^2) to obtain the best fitted curve. Both the determination coefficient (R^2) and reduced chi-square (χ^2_{red}) [Eq. (18)] were adopted to evaluate the quality of the NLR and define the best kinetic model describing the adsorption kinetics.

$$w_i = \frac{1}{y_i} \quad (17)$$

where w_i is the weighting coefficient and y_i is the experimental data point

$$\chi^2_{red} = \frac{\sum_{i=1}^{N} w_i (y_i - \hat{y}_i)^2}{\upsilon} \quad (18)$$

where $\hat{y}_i$ is the estimated data point calculated by the model and υ $(N - P)$ is the number of degrees of freedom, which depends on the number of experimental data points (N) and number of variables (P) of the model used for NLR analysis.

The experimental results of the adsorption study as a function of contact time and the generated curves by the modeling the experimental data with pseudo-first and second-order models are shown in Fig. 4a–d. Table 2 presents the results of modeling the experimental data with pseudo-first and second-order kinetic models. As seen in Fig. 4a–d, the adsorption equilibrium time was attained after 360 min for Co^{2+}, Cu^{2+}, and Ni^{2+} and 720 min for Cr^{6+}. Table 2 also shows that when comparing the values of $q_{e,exp}$ with $q_{e,calc}$ and R^2 and χ^2_{red} for both pseudo-first and second-order models, it is possible to suggest that the adsorption of Co^{2+}, Cu^{2+}, and Ni^{2+} is better described by a pseudo-first-order kinetic model, whereas the adsorption of Cr^{6+} is better described by a pseudo-second-order kinetic model.

3.2.2. Effect of solution pH

The effect of the solution pH on removal of Co^{2+}, Cu^{2+}, Ni^{2+}, and Cr^{6+} species was evaluated at 25 °C, 150 rpm, 0.2 g/L C2 adsorbent, and 100 mg/L Cu^{2+}, 70 mg/L Co^{2+} and Ni^{2+}, and 25 mg/L Cr^{6+}. The equilibrium times used in these studies are presented in Table 2 and were taken with basis on the kinetic study (Section 3.2.1). Fig. 5 shows the equilibrium adsorption capacity (q_e) of Co^{2+}, Cu^{2+}, Ni^{2+}, and Cr^{6+} on the C2 adsorbent as a function of the solution pH from 2.0 to 5.5 for Cu^{2+}, from 3.0 to 6.0 for Co^{2+}, from 2.0 to 7.5 for Ni^{2+}, and from 2.0 to 7.5 for Cr^{6+}. The C2 adsorbent may have amphoteric features as it has permanent positive charges on the quaternary ammonium groups at C-2 of the pyranosidic ring, which are pH-independent, pH-dependent charges of tertiary amine groups on the EDTA moiety (pK_a values of amine groups of EDTA are equal to 6.13 and 10.37) [32] and non-quaternized amine groups at C-2, and pH-dependent charges on carboxylic groups in the EDTA moiety (the pK_a values of the carboxylic groups of EDTA are equal to 0.0, 1.5, 2.0, and 2.69) [32]. Due to the speciation of these chemical groups with changes in the solution pH, the pH is one of most important parameters for controlling the adsorption of metallic cationic and/or anionic species in aqueous solution using C2 as the adsorbent. As seen in Fig. 5, the adsorption of metallic cations Co^{2+}, Cu^{2+}, and Ni^{2+} increased as the pH was increased and reached a maximum at a pH value of 4.5 for $Co^{2+}$and Cu^{2+} and 7.5 for Ni^{2+}. The PZC of the C2 adsorbent was found to be 4.8. Thus, the adsorption of cationic species such as metallic cations was favored at pH > PZC, where the C2 adsorbent has a net negative charge. The high adsorption capacity of C2 at low pH values (pH 2–3) is related to the acidic properties of the iminoacetate and iminodiacetate groups of the EDTA moiety (the pK_a values of EDTA are equal to 0.0, 1.5, 2.0, and 2.69). The permanent positive charges of the quaternary ammonium groups at C-2 do not seem to have reduced the adsorption capacity of metallic cationic species on the C2 adsorbent. This result may be explained by the high affinity of the EDTA moiety for complex metallic cations, which has been previously demonstrated [21] by investigating the adsorption of Cd^{2+}, Cu^{2+}, and Pb^{2+} on mercerized cellulose and mercerized sugarcane bagasse chemically modified with EDTAD.

The oxyanions of Cr^{6+} may be present in aqueous solution in neutral and/or anionic forms as a function of the solution pH, ionic strength, and concentration, as described by the following equilibria [33]:

$$H_2CrO_4 + H_2O \rightleftharpoons H_3O^+ + HCrO_4^- \quad (K = 4.1)$$

$$HCrO_4^- + H_2O \rightleftharpoons H_3O^+ + CrO_4^{2-} \quad (K = 10^{-5.9})$$

$$2HCrO_4^- \rightleftharpoons Cr_2O_7^{2-} + H_2O + \quad (K = 10^{-2.2})$$

$$HCr_2O_7^- + H_2O \rightleftharpoons H_3O^+ + Cr_2O_7^{2-} \quad (K = 10^{-8.5})$$

Supplementary Fig. 1 shows the speciation diagram for species of oxyanions of Cr^{6+} as a function of the solution pH (ionic strength of 0.1 mol/L and 25 mg/L or 0.48 mmol/L Cr(VI)) calculated using Hydra and Medusa software. At pH values from 2 to 5, $HCrO_4^-$ and $Cr_2O_7^{2-}$ are the main species in equilibrium with a predominance of $HCrO_4^-$ over $Cr_2O_7^{2-}$. At pH values lower than 1, H_2CrO_4 and $HCrO_4^-$ are the predominant species. At pH 6, $HCrO_4^-$ and CrO_4^{2-} are in equilibrium with the fraction of both species being close to 50%. At pH values higher than 7, CrO_4^{2-} is the predominant form [34]. As seen in Fig. 5, the adsorption of oxyanions of Cr^{6+} increased as the pH was decreased and reached a maximum at pH close to 2. In this condition, tertiary amines of the EDTA moiety and non-quaternized amines at C-2 are protonated and positively charged, contributing to the adsorption of oxyanions of Cr^{6+} through electrostatic interactions, while the quaternary ammonium groups at C-2 with permanent positive charges also contribute to increase the adsorption of oxyanions of Cr^{6+} through an ion exchange process with the consequent release of I^- to the aqueous solution. The explanation for the decrease in the adsorption capacity as the pH was increased is related to the partial deprotonation of tertiary amines of the EDTA moiety and non-quaternized amines at C-2 and an increase in the presence of CrO_4^{2-} species above pH 5, which requires two positively charged adsorption sites to be adsorbed by the C2 adsorbent. These results agree with the value of PZC.

3.2.3. Adsorption isotherms

Adsorption isotherms describe how different types of adsorbates can interact with an adsorbent and are important in the optimization of the use of an adsorbent in a real wastewater treatment plant based on the adsorption process. Various isotherm models are available in the literature [35]. Thus, three of the most widely

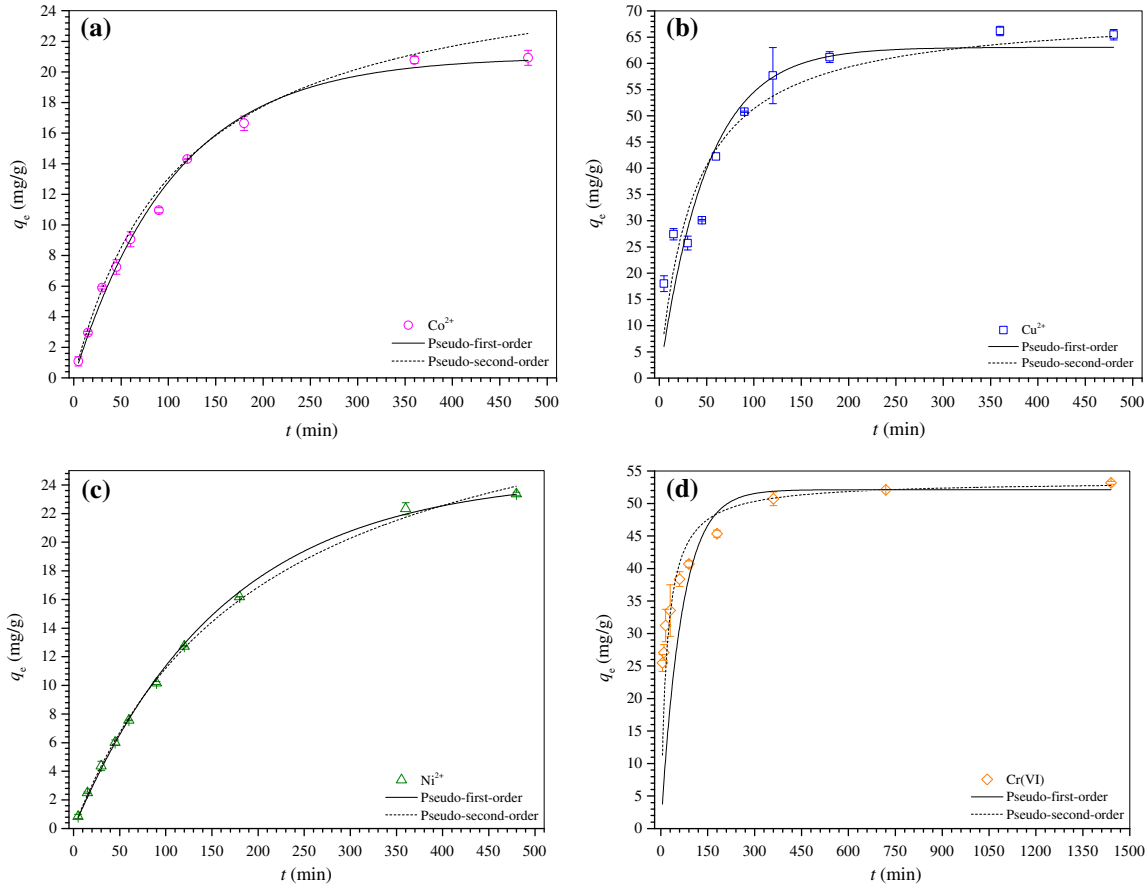

Fig. 4. Effect of contact time on adsorption of (a) Co^{2+}, (b) Cu^{2+}, (c) Ni^{2+}, and (d) Cr^{6+} on C2 at 25 °C, 150 rpm, 0.2 g/L C2, pH 4.5 for Co^{2+} and Cu^{2+}, 7.5 for Ni^{2+}, and 2.0 for Cr^{6+}, and 20 mg/L for Co^{2+} and Ni^{2+}, 70 mg/L for Cu^{2+}, and 25 mg/L for Cr^{6+}.

Table 2
Modeled kinetic parameters for the adsorption of Co^{2+}, Cu^{2+}, Ni^{2+}, and Cr^{6+} on C2.

Parameters	Co^{2+}	Cu^{2+}	Ni^{2+}	Cr^{6+}
$C_{i,M^{n+}}$ (mg/L)	20	70	20	25
t_e (min)	360	360	360	720
pH	4.5	4.5	7.5	2.0
$q_{e,exp}$ (mg/g)	20.85 ± 0.10	65.82 ± 0.49	22.86 ± 0.73	52.64 ± 0.75
$q_{e,exp}$ (mmol/g)	0.354 ± 0.002	1.036 ± 0.008	0.389 ± 0.012	1.012 ± 0.014
Pseudo-first-order				
k_1 (min^{-1})	$(9.43 \pm 0.54) \times 10^{-3}$	$(2.00 \pm 0.50) \times 10^{-2}$	$(6.20 \pm 0.24) \times 10^{-3}$	$(1.50 \pm 0.32) \times 10^{-2}$
$q_{e,calc}$ (mg/g)	20.98 ± 0.61	63.06 ± 6.19	24.61 ± 0.53	52.11 ± 0.28
$q_{e,calc}$ (mmol/g)	0.356 ± 0.010	0.992 ± 0.097	0.419 ± 0.009	1.002 ± 0.005
R^2	0.9954	0.7799	0.9984	0.5340
χ^2_{red}	0.0304	1.8690	0.0113	94.9571
Pseudo-second-order				
k_2 (g/mg.min)	$(3.17 \pm 0.44) \times 10^{-4}$	$(3.91 \pm 1.56) \times 10^{-4}$	$(1.43 \pm 0.01) \times 10^{-4}$	$(1.00 \pm 0.28) \times 10^{-3}$
$q_{e,calc}$ (mg/g)	27.83 ± 1.25	70.11 ± 7.22	34.10 ± 0.81	53.45 ± 0.41
$q_{e,calc}$ (mmol/g)	0.472 ± 0.021	1.103 ± 0.114	0.581 ± 0.014	1.028 ± 0.008
R^2	0.9964	0.8345	0.9990	0.8319
χ^2_{red}	11.8960	1.4057	0.0075	34.2474

used isotherms were chosen to evaluate the equilibrium adsorption data: the Langmuir, Freundlich, and Langmuir–Freundlich (Sips) isotherms.

The Langmuir [36] isotherm theory assumes the formation of a monolayer of adsorbate on the homogeneous surface of the adsorbent. In addition, adsorption occurs at specific sites on the homogeneous surface of the adsorbent. Once an adsorbate occupies a site, there can be no adsorption there. The Langmuir isotherm can be presented by Eq. (19) as follows:

$$q_e = \frac{Q_{max} b C_e}{1 + b C_e} \quad (19)$$

where q_e (mg/g) is the equilibrium adsorption capacity, Q_{max} (mg/g) is the maximum amount of adsorbate per unit weight of the C2 to form a complete monolayer coverage on the surface bound at a high equilibrium adsorbate concentration, C_e (mg/L), and b (L/mg) is the Langmuir constant related to the affinity of the adsorbate at the binding sites.

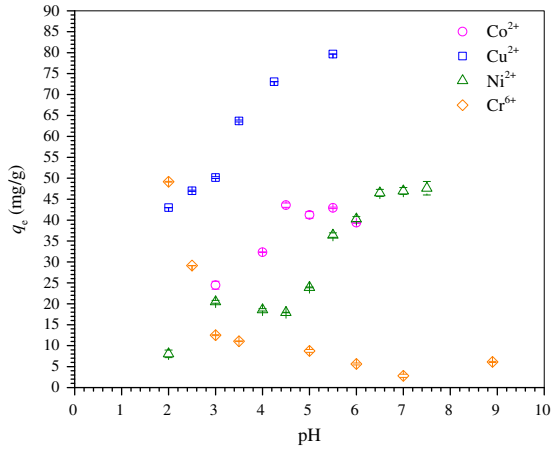

Fig. 5. Effect of the solution pH on adsorption of Co^{2+}, Cu^{2+}, Ni^{2+}, and Cr^{6+} on C2 at 25 °C, 150 rpm, 0.2 g/L C2, 70 mg/L Co^{2+} and Ni^{2+}, 100 mg/L Cu^{2+}, and 25 mg/L Cr^{6+}, and 360 min of contact time for Co^{2+}, Cu^{2+}, and Ni^{2+} and 720 min for Cr^{6+}.

One of the essential characteristics of the Langmuir isotherm can be expressed by a separation factor, R_L; which is defined by Eq. (20) as follows:

$$R_L = \frac{1}{1 + bC_i} \tag{20}$$

where C_i is the initial concentration of adsorbate. The value of R_L indicates if an isotherm is irreversible ($R_L = 0$), favorable ($0 < R_L < 1$), linear ($R_L = 1$), or unfavorable ($R_L > 1$).

The Freundlich [37] isotherm is an empirical equation which is applicable to adsorption on heterogeneous surfaces and is not restricted to the formation of a monolayer. It assumes that an increase in the adsorbate concentration also increases the amount of the adsorbate adsorbed on the surface. It can be represented by Eq. (21) as follows:

$$q_e = K_F C_e^{1/n} \tag{21}$$

where K_F [mg/g(L/mg)$^{1/n}$] and n are the Freundlich constants. The parameter n is usually greater than unity and it is related to the adsorption intensity.

Sips [38] recognized the problem of the continuing, infinite increase in adsorption capacity with increasing the concentration of the adsorbate in the Freundlich isotherm. Thus, Sips proposed an isotherm equation similar in form to the Freundlich isotherm, but with a finite limit when the concentration is sufficiently high, as shown in Eq. (22):

$$q_e = Q_{max} \frac{(bC_e)^{1/n}}{1 + (bC_e)^{1/n}} \tag{22}$$

The Langmuir–Freundlich (Sips) isotherm resembles the Langmuir isotherm. The difference between the Sips and Langmuir isotherms is the additional parameter n in the Sips isotherm. If the parameter n is unity, the Sips isotherm reduces to the Langmuir isotherm and is applicable to ideal surfaces. Thus, the parameter n can be considered as a parameter characterizing the heterogeneity of the adsorption system.

The change in free energy ($\Delta_{ads}G°$) of an adsorption system can be calculated using Eq. (23) as follows:

$$\Delta_{ads}G^{\circ} = -RT \ln K_a \tag{23}$$

where K_a is the thermodynamic equilibrium constant (dimensionless), T (K) is the absolute temperature, and R (8.314 J/K mol) is the ideal gas constant.

The thermodynamic equilibrium constant can be calculated from the Langmuir constant, b, using the approach suggested by Liu [39] in Eq. (24) as follows:

$$K_a = \left[\frac{b}{\gamma_e}(1\ \text{mol/L})\right] \tag{24}$$

where γ_e is the activity coefficient in the equilibrium (dimensionless) at 25 °C.

If the adsorbate is a metallic ion, the activity coefficient is strongly affected and it sharply decreases as the ionic strength increases. Therefore, it is fundamental to correct the activity coefficient for each adsorption system using the extended Debye Hückel law [Eq. (25)] to provide a correct calculation of $\Delta_{ads}G°$ as follows [39]:

$$\log \gamma_e = \frac{-0.509 z^2 \sqrt{I_e}}{1 + \alpha \sqrt{I_e/305}} \tag{25}$$

where z is the charge of the metallic ion, I_e (mol/L) is the ionic strength, and α (pm) is the hydrated ion size (600 pm for Co^{2+}, Cu^{2+}, and Ni^{2+} and 900 pm for oxyanions of Cr^{6+}) [40]. The ionic strength was calculated taking into account the first equilibrium concentration data point of the plateau of the adsorption isotherms [41].

The isotherms for the adsorption of Co^{2+}, Cu^{2+}, Ni^{2+}, and oxyanions of Cr^{6+} on C2 at 25 °C, 150 rpm, 0.2 g/L C2, pH 4.5 for Co^{2+} and Cu^{2+}, 7.5 for Ni^{2+}, and 2.0 for Cr^{6+}, and 360 min of contact time for Co^{2+}, Cu^{2+}, and Ni^{2+} and 720 min for oxyanions of Cr^{6+} are presented in Fig. 6a–d. The adsorption isotherms were modeled by NLR analysis of the experimental data (Supplementary Table 2) using Microcal Origin® 2015 software and the isotherm models of Langmuir, Freundlich, and Sips. The isotherm model parameters were found by minimizing the χ^2_{red}. The routines used to model the experimental data using the isotherm models were the same as those described in Section 3.2.1. Table 3 shows the results. As seen in Table 3, the values of R_L for all adsorption systems were between 0 and 1, indicating that the adsorption isotherms of Co^{2+}, Cu^{2+}, Ni^{2+}, and oxyanions of Cr^{6+} on C2 were favorable.

As seen in Table 3, considering the values of $Q_{max,exp}$, R^2, and χ^2_{red} and the shape of the isotherm curves presented in Fig. 6a–d, the adsorption of Co^{2+} and Ni^{2+} was best described by the Langmuir model, while the adsorption of Cu^{2+} and oxyanions of Cr^{6+} was best described by the Sips model. The parameter n of the Sips model also suggests that the adsorption system involving the adsorption of Cu^{2+} and oxyanions of Cr^{6+} on C2 adsorbent are more heterogeneous, whereas the value of n for the adsorption of Co^{2+} and Ni^{2+} on C2 demonstrates that these adsorption systems are more Langmuirian than Freundlichian, i.e. less heterogeneous. In fact, the C2 adsorbent has a heterogeneous surface, as the sites of adsorption are mostly composed of carboxylic, tertiary amine, and quaternary ammonium groups. Thus, the surface of the C2 adsorbent is not comprised of adsorption sites with identical energy and affinity to the different types of adsorbates studied. Thus, although the Langmuir model failed to completely describe the adsorption systems studied, its use is valid to estimate the adsorption constants for comparison purposes. Furthermore, the deviations may be computed using the Sips model through the evaluation of the value of the parameter n.

According to the equilibrium experimental adsorption data and the Langmuir and Sips models, the experimental maximum adsorption capacity ($Q_{max,exp}$) and calculated maximum adsorption capacity (Q_{max}) for the C2 adsorbent were in the following order $Cr^{6+} \gg Cu^{2+} > Ni^{2+} > Co^{2+}$. These results demonstrate the efficacy of the C2 adsorbent to remove both inorganic cationic and anionic species from aqueous solutions.

The Pearson parameters (δ) for Co^{2+}, Ni^{2+}, and Cu^{2+} are 0.130, 0.126, and 0.104 [42], respectively. Thus, the hardness order of

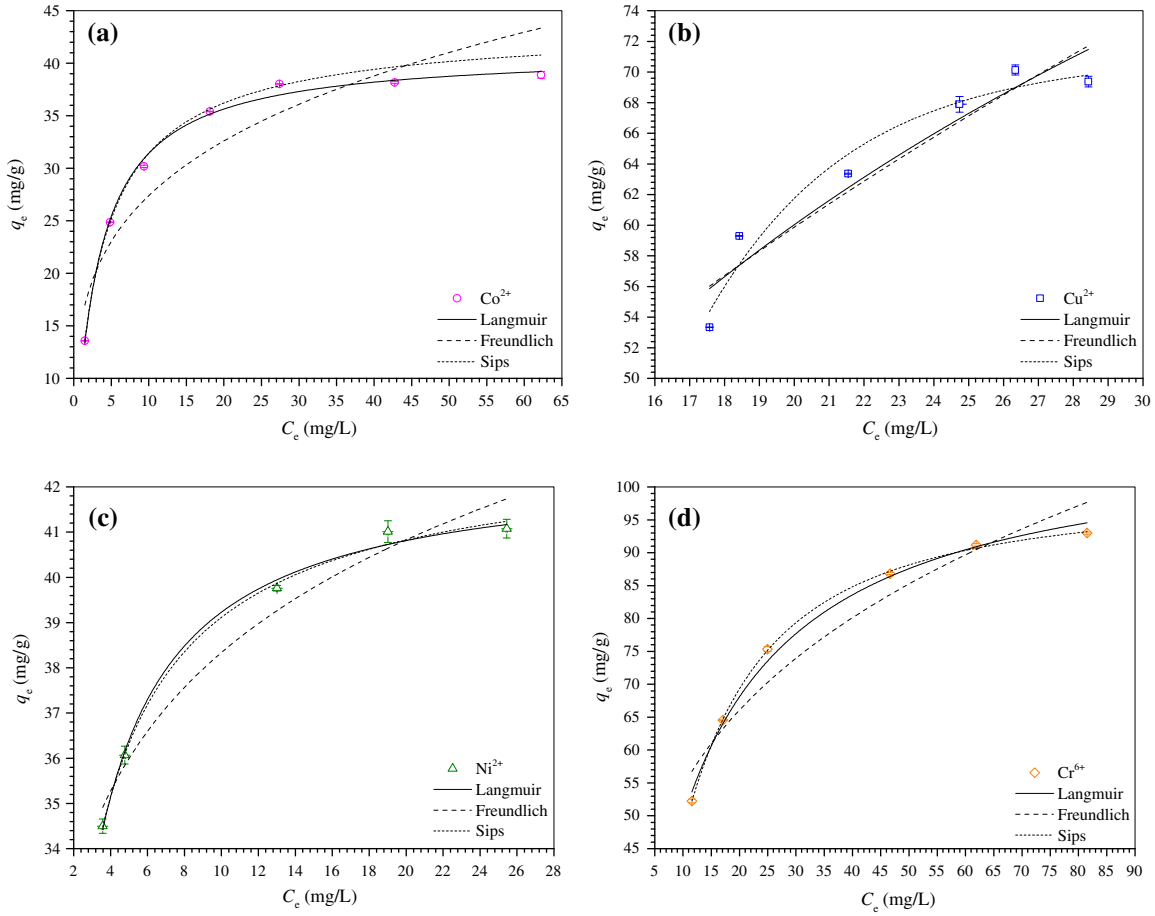

Fig. 6. Adsorption isotherms for (a) Co^{2+}, (b) Cu^{2+}, (c) Ni^{2+}, and Cr^{6+} on C2 at 25 °C, 150 rpm, 0.2 g/L C2, pH 4.5 for Co^{2+} and Cu^{2+}, 7.5 for Ni^{2+}, and 2.0 for Cr^{6+}, and 360 min of contact time for Co^{2+}, Cu^{2+}, and Ni^{2+} and 720 min for Cr^{6+}.

Table 3
Modeled isotherm parameters for the adsorption of Co^{2+}, Cu^{2+}, Ni^{2+}, and Cr^{6+} on C2 adsorbent.

	Co^{2+}	Cu^{2+}	Ni^{2+}	Cr^{6+}
$Q_{max,exp}$ (mg/g)	37.15 ± 2.46	69.75 ± 0.54	41.04 ± 0.05	92.09 ± 1.28
$Q_{max,exp}$ (mmol/g)	0.630 ± 0.042	1.098 ± 0.008	0.699 ± 0.001	1.771 ± 0.025
pH	4.5	4.5	7.5	2.0
t_e (min)	360	360	360	720
I_e (mol/L)	0.1022	0.1012	0.4010	0.4011
γ_e	0.882	0.882	0.878	0.978
Langmuir				
Q_{max} (mg/g)	41.15 ± 0.45	130.38 ± 20.52	42.53 ± 0.18	108.22 ± 1.89
Q_{max} (mmol/g)	0.698 ± 0.008	2.052 ± 0.323	0.725 ± 0.003	2.081 ± 0.036
b (L/mg)	0.323 ± 0.015	0.043 ± 0.013	1.189 ± 0.047	0.085 ± 0.005
b (L/mol)	19047.3 ± 855.6	2711.2 ± 841.6	69771.4 ± 2737.9	4413.7 ± 265.1
R^2	0.9972	0.9004	0.9954	0.9927
χ^2_{red}	0.0119	0.0725	0.0011	0.0283
R_L	0.424–0.042	0.456–0.358	0.074–0.024	0.349–0.105
K_a	21584.9 ± 969.6	3072.2 ± 953.6	79494.1 ± 3119.4	4509.3 ± 270.9
$\Delta_{ads}G°$ (kJ/mol)	−24.74 ± 1.11	−19.91 ± 6.18	−27.97 ± 1.10	−20.86 ± 1.25
Freundlich				
K_F [mg/g(L/mg)$^{1/n}$]	15.37 ± 2.02	12.88 ± 3.36	31.09 ± 0.69	28.71 ± 3.74
n	3.984 ± 0.664	1.949 ± 0.319	10.995 ± 1.076	3.594 ± 0.461
R^2	0.8845	0.8851	0.9640	0.9287
χ^2_{red}	0.4966	0.0837	0.0088	0.2777
Sips				
Q_{max} (mg/g)	43.86 ± 0.68	71.48 ± 3.30	43.11 ± 1.19	99.32 ± 0.88
Q_{max} (mmol/g)	0.744 ± 0.012	1.125 ± 0.052	0.735 ± 0.020	1.910 ± 0.017
b (L/mg)	0.278 ± 0.012	0.071 ± 0.006	1.376 ± 0.368	0.093 ± 0.001
b (L/mol)	16402.2 ± 676.7	4490.0 ± 354.7	80748.8 ± 21591.5	4852.2 ± 57.4
n	1.104 ± 0.035	0.187 ± 0.086	1.149 ± 0.289	0.746 ± 0.026
R^2	0.9993	0.9426	0.9941	0.9995
χ^2_{red}	150.3196	0.0418	0.0014	0.0019

Table 4
Comparison of Q_{max} for removal of Co^{2+}, Cu^{2+}, Ni^{2+}, and Cr^{6+} by various modified chitosan adsorbents reported in the literature.

Adsorbent abbreviation or name	Type of solid support	Ligand type	pH	Equilibrium time (min)	Q_{max} (mg/g) at 25 °C				References
					Co^{2+}	Cu^{2+}	Ni^{2+}	Cr^{6+}	
Cross-linked chitosan	Chitosan	Amine(R-NH_2)/alkylated amine (R-NH-R′)	5	–	–	80.0	–	78.0	[44]
Ch-g-Aam	Chitosan	Carboxylic acid/amine/amide	6 for Cu^{2+} and 4 for Cr^{6+}	1440	–	166.0	–	935.0	[45]
Ch-g-Aa	Chitosan	Carboxylic acid/amine/amide	6 for Cu^{2+} and 4 for Cr^{6+}	1440	–	318.0	–	518.0	[45]
Aminated chitosan	Chitosan	Amine (R-NH-R′ and R-NH_2)	–	720	–	–	30.2	28.7	[46]
Ch-g-NCB	Chitosan	Carboxylic acid/amine/imine/phosphate	5	1440	–	308.0	321.0	175.0	[47]
C2	Chitosan	Carboxylic acid/amine/quaternary ammonium	4.5 for Co^{2+} and Cu^{2+}, 7.5 for Ni^{2+}, and 2 for Cr^{6+}	360 for Co^{2+}, Cu^{2+}, and Ni^{2+} and 720 for Cr^{6+}	41.2	71.5	42.5	99.3	This study

the metal ions is in the order $Co^{2+} > Ni^{2+} > Cu^{2+}$. The carboxylic and amine groups of the grafted EDTA moiety and non-quaternized amine groups at C-2 of the pyranosidic ring on the C2 adsorbent behave as hard bases. From the point of view of the hard and soft acid base (HSAB) concept, these ligands should exhibit a preference for hard acid metal ions following the hardness order $Co^{2+} > Ni^{2+} > Cu^{2+}$. However, according to the series of Irving and Williams [43], which discusses the relative stabilities of complexes formed by metal ions with various ligands, carboxylic and amines form more stable complexes with the studied metal ions in the following stability order $Cu^{2+} > Ni^{2+} > Co^{2+}$. This order may also be explained by the general stability sequence of high spin octahedral metal ion complexes using the Irving–Williams series concept [43]. Therefore, the results of Q_{max} obtained in this study are in good agreement with the concept of Irving and Williams.

The values of $\Delta_{ads}G^{\circ}$ for adsorption of Co^{2+}, Cu^{2+}, Ni^{2+}, and oxyanions of Cr^{6+} are in the range from −20 to −28 kJ/mol. It is suggested that a mixed mechanism may be controlling the uptake of Co^{2+}, Cu^{2+}, Ni^{2+}, and oxyanions of Cr^{6+} on the C2 adsorbent from aqueous solutions. As seen in Fig. 1, the process of removing oxyanions of Cr^{6+} from aqueous solution is suggested to be ion exchange, where an iodine anion is exchanged by an oxyanion of Cr^{6+}. In addition, the non-quaternized nitrogen atoms at the C-2 position of the pyranosidic ring and tertiary amines of the EDTA moiety may remove Co^{2+}, Cu^{2+}, and Ni^{2+} ions from aqueous solution through complexation, while the carboxylic groups of the EDTA moiety may remove Co^{2+}, Cu^{2+}, and Ni^{2+} ions from aqueous solution through ion exchange, where a sodium or a hydronium ion may be exchanged by a metal ion.

3.3. Desorption and reuse of the C2 adsorbent

The desorption efficiencies (E_{des}) for Co^{2+}, Cu^{2+}, Ni^{2+}, and Cr^{6+} were 86.7, 22.4, 31.2, and 46.9%. Therefore, E_{des} presented the following order $Co^{2+} > Cr^{6+} > Ni^{2+} > Cu^{2+}$. This means that Cu^{2+} and Ni^{2+} are strongly complexed by EDTA moiety on the C2 adsorbent, thereby making it difficult to desorb. In contrast, Co^{2+} was easier desorbed in comparison with Cu^{2+} and Ni^{2+}. The mechanism of desorption of Co^{2+}, Cu^{2+}, and Ni^{2+} is expected to be ion exchange, where Co^{2+}, Cu^{2+}, or Ni^{2+} ions are exchanged by hydronium ions. It seems that the stability constant (β) for the formation of a complex between EDTA moiety and metal ions is the limiting factor hampering an extensive desorption of Cu^{2+} and Ni^{2+}.

The desorption mechanism of oxyanions of Cr^{6+} is also expected to be ion exchange. However, in this case oxyanions of Cr^{6+} such as $HCrO_4^-$ and $Cr_2O_7^{2-}$, are exchanged by nitrate ions (NO_3^-). These results demonstrated that one type of desorption solution could be used to desorb both metal cations and oxyanions of Cr^{6+}, thereby decreasing the costs for desorption and recovery of both the C2 adsorbent and adsorbates.

The re-adsorption efficiencies (*RE*) for Co^{2+}, Cu^{2+}, Ni^{2+}, and Cr^{6+} were 87.0, 112.4, 113.0, and 141.7%. It is noticed that *RE* for Co^{2+} is less than 100%, which means that the C2 adsorbent lost part of its adsorption capacity for Co^{2+} after the first cycle of adsorption–desorption. However, the *RE* for Cu^{2+}, Ni^{2+}, and Cr^{6+} were higher than 100%, which means that the C2 adsorbent is capable of adsorbing more Cu^{2+}, Ni^{2+}, and Cr^{6+} after one cycle of adsorption–desorption. It seems that after the first cycle of adsorption–desorption the surface of the C2 adsorbent presents more affinity for these metal ions and oxyanions. These results demonstrated that even the C2 adsorbent is not being fully desorbed it may be recovered and reused in a new cycle of adsorption as it still presents ability to adsorb metal ions and oxyanions of Cr^{6+}.

3.4. Comparison of the C2 adsorbent with other adsorbents available in the literature for the same purpose

Table 4 shows various adsorbent materials prepared from chitosan using different synthesis/modifications strategies for the removal of Co^{2+}, Cu^{2+}, Ni^{2+}, and Cr^{6+} from aqueous solutions in batch mode for comparison purposes. Comparing the C2 adsorbent with some previously reported adsorbents in the literature, it is possible to suggest that C2 has some advantages and disadvantages. The main disadvantage is the smaller adsorption capacity in comparison with Ch-g-Aam, Ch-g-Aa, and Ch-g-NCB adsorbents, while the major advantages are the versatility of C2 to adsorb a reasonable amount of Co^{2+}, Cu^{2+}, Ni^{2+}, and Cr^{6+} in a larger pH range and with shorter equilibrium times due to the chemical characteristics of the groups grafted onto C2.

4. Conclusions

Chitosan was successfully modified with methyl iodide and EDTA dianhydride to produce a new bifunctionalized adsorbent (C2) capable of removing cationic and anionic species by adsorption. C2 was characterized by elemental analysis, FTIR, and SS ^{13}C NMR. The C2 adsorbent was effective in removing Co^{2+}, Cu^{2+}, Ni^{2+}, and oxyanions of Cr^{6+} from aqueous solutions. The adsorption of Co^{2+}, Cu^{2+}, and Ni^{2+} followed the pseudo-first-order kinetic model, while the adsorption of oxyanions of Cr^{6+} followed the pseudo-second-order model. The equilibrium adsorption times were found to be 360 min for Co^{2+}, Cu^{2+}, and Ni^{2+} and 720 min for oxyanions of Cr^{6+}. The adsorption isotherms of Co^{2+} and Ni^{2+} were best described by the Langmuir model, whereas the isotherms of Cu^{2+} and oxyanions of Cr^{6+} were best described by the Sips model. The maximum adsorption capacities (Q_{max}) were

0.698, 1.125, 0.725, and 1.910 mmol/g for Co^{2+}, Cu^{2+}, Ni^{2+}, and Cr^{6+}, respectively. The $\Delta_{ads}G^{\circ}$ were in the range from −20 to −28 kJ/mol. C2 adsorbents loaded with Co^{2+}, Cu^{2+}, $Ni^{2+}$and Cr^{6+} were desorbed with 0.1 mol/L HNO_3. The desorption efficiencies were 86.7%, 22.4%, 31.2%, and 46.9%. C2 adsorbents were recovered and subjected to re-adsorption studies, which showed that these adsorbents can still adsorb both metallic cations and oxyanions of Cr^{6+} with certain efficiency.

Acknowledgments

The authors are grateful to Universidade Federal de Ouro Preto (UFOP), Universidade Federal de Minas Gerais (UFMG), Fundação de Amparo à Pesquisa do Estado de Minas Gerais (FAPEMIG Grant Numbers CEX APQ-01945/13 and CEX APQ-01764/14), and Conselho Nacional de desenvolvimento Científico (CNPq Grant Number 448346/2014-1) for funding this research. The authors are also grateful to Coordenação de Aperfeiçoamento de Pessoal de Nível Superior (CAPES) (for a doctoral scholarship awarded to B. C.S. Ferreira) and FAPEMIG (for an undergraduate scholarship awarded to A.L.S.L. Moreira).

Appendix A. Supplementary material

Supplementary data associated with this article can be found, in the online version, at http://dx.doi.org/10.1016/j.jcis.2015.12.037.

References

[1] W.S. Wan Ngah, L.C. Teong, M.A.K.M. Hanafiah, Adsorption of dyes and heavy metal ions by chitosan composites: a review, Carbohydr. Polym. 83 (4) (2011) 1446–1456.
[2] S.K. Kim, Chitin, Chitosan, Oligosaccharides and Their Derivatives: Biological Activities and Applications, CRC Press, New York, USA, 2010.
[3] E.P. Ageev, N.N. Matushkina, Peculiarities of the transport properties of chitosan films. 1. Concentration prehistory of pervaporation, Colloid J. 77 (3) (2015) 251–255.
[4] Z. Hao, Y. Cai, X. Liao, X. Zhang, Z. Fang, D. Zhang, Optimization of nutrition factors on chitinase production from a newly isolated Chitiolyticbacter meiyuanensis SYBC-H1, Braz. J. Microbiol. 43 (1) (2012) 177–186.
[5] F.-C. Wu, R.-L. Tseng, R.-S. Juang, A review and experimental verification of using chitosan and its derivatives as adsorbents for selected heavy metals, J. Environ. Manage. 91 (4) (2010) 798–806.
[6] A.J. Varma, S.V. Deshpande, J.F. Kennedy, Metal complexation by chitosan and its derivatives: a review, Carbohydr. Polym. 55 (1) (2004) 77–93.
[7] C. Gerente, V.K.C. Lee, P.L. Cloirec, G. McKay, Application of chitosan for the removal of metals from wastewaters by adsorption—mechanisms and models review, Crit. Rev. Environ. Sci. Technol. 37 (1) (2007) 41–127.
[8] P. Miretzky, A.F. Cirelli, Hg(II) removal from water by chitosan and chitosan derivatives: a review, J. Hazard. Mater. 167 (1–3) (2009) 10–23.
[9] A. Bhatnagar, M. Sillanpää, Applications of chitin- and chitosan-derivatives for the detoxification of water and wastewater—a short review, Adv. Colloid Interface Sci. 152 (1–2) (2009) 26–38.
[10] G.Z. Kyzas, D.N. Bikiaris, Recent modifications of chitosan for adsorption applications: a critical and systematic review, Mar. Drugs 13 (1) (2015) 312–337.
[11] V.M. Boddu, K. Abburi, J.L. Talbott, E.D. Smith, R. Haasch, Removal of arsenic (III) and arsenic (V) from aqueous medium using chitosan-coated biosorbent, Water Res. 42 (3) (2008) 633–642.
[12] V.A. Spinelli, M.C.M. Laranjeira, V.T. Fávere, Preparation and characterization of quaternary chitosan salt: adsorption equilibrium of chromium(VI) ion, React. Funct. Polym. 61 (3) (2004) 347–352.
[13] W.E. Marshall, L.H. Wartelle, Chromate (CrO_4^{2-}) and copper (Cu^{2+}) adsorption by dual-functional ion exchange resins made from agricultural by-products, Water Res. 40 (13) (2006) 2541–2548.
[14] R. Laus, T.G. Costa, B. Szpoganicz, V.T. Fávere, Adsorption and desorption of Cu (II), Cd(II) and Pb(II) ions using chitosan crosslinked with epichlorohydrin–triphosphate as the adsorbent, J. Hazard. Mater. 183 (1–3) (2010) 233–241.
[15] P.O. Boamah, Y. Huang, M. Hua, Q. Zhang, J. Wu, J. Onumah, L.K. Sam-Amoah, P. O. Boamah, Sorption of heavy metal ions onto carboxylate chitosan derivatives—a mini-review, Ecotoxicol. Environ. Saf. 116 (2015) 113–120.
[16] M. Salman, M. Athar, U. Farooq, Biosorption of heavy metals from aqueous solutions using indigenous and modified lignocellulosic materials, Rev. Environ. Sci. Bio/Technol. (2015) 1–18.
[17] F. Fu, Q. Wang, Removal of heavy metal ions from wastewaters: a review, J. Environ. Manage. 92 (3) (2011) 407–418.
[18] C. Klaassen, Casarett & Doull's Toxicology: The Basic Science of Poisons: The Basic Science of Poisons, McGraw-Hill, New York, 2008.
[19] M.A. Barakat, New trends in removing heavy metals from industrial wastewater, Arab. J. Chem. 4 (4) (2011) 361–377.
[20] Ö.V. Rúnarsson, J. Holappa, T. Nevalainen, M. Hjálmarsdóttir, T. Järvinen, T. Loftsson, J.M. Einarsson, S. Jónsdóttir, M. Valdimarsdóttir, M. Másson, Antibacterial activity of methylated chitosan and chitooligomer derivatives: synthesis and structure activity relationships, Eur. Polym. J. 43 (6) (2007) 2660–2671.
[21] O. Karnitz, L.V.A. Gurgel, R.P. de Freitas, L.F. Gil, Adsorption of Cu(II), Cd(II), and Pb(II) from aqueous single metal solutions by mercerized cellulose and mercerized sugarcane bagasse chemically modified with EDTA dianhydride (EDTAD), Carbohydr. Polym. 77 (3) (2009) 643–650.
[22] J. Brugnerotto, J. Lizardi, F. Goycoolea, W. Argüelles-Monal, J. Desbrieres, M. Rinaudo, An infrared investigation in relation with chitin and chitosan characterization, Polymer 42 (8) (2001) 3569–3580.
[23] J.S. Noh, J.A. Schwarz, Effect of HNO_3 treatment on the surface-acidity of activated carbons, Carbon 28 (5) (1990) 675–682.
[24] W.M. Haynes, CRC Handbook of Chemistry and Physics, Taylor & Francis, 2014.
[25] V.K. Mourya, N. Inamdar, Trimethyl chitosan and its applications in drug delivery, J. Mater. Sci.: Mater. Med. 20 (5) (2009) 1057–1079.
[26] I. Kavianinia, P.G. Plieger, N.G. Kandile, D.R.K. Harding, Fixed-bed column studies on a modified chitosan hydrogel for detoxification of aqueous solutions from copper (II), Carbohydr. Polym. 90 (2) (2012) 875–886.
[27] V. Balsamo, F. López-Carrasquero, E. Laredo, K. Conto, J. Contreras, J.L. Feijoo, Preparation and thermal stability of carboxymethyl starch/quaternary ammonium salts complexes, Carbohydr. Polym. 83 (4) (2011) 1680–1689.
[28] S. Aime, R. Gobetto, R. Nano, E. Santucci, ^{13}C solid state CP/MAS NMR studies of EDTA complexes, Inorg. Chim. Acta 129 (2) (1987) L23–L25.
[29] Y.S. Ho, G. McKay, Pseudo-second order model for sorption processes, Process Biochem. 34 (5) (1999) 451–465.
[30] S.Y. Lagergren, Zur Theorie der sogenannten Adsorption gelöster Stoffe, Kungliga Svenska Vetenskapsakademiens, Handlingar 24 (4) (1898) 1–39.
[31] Y.S. Ho, G. McKay, Kinetic models for the sorption of dye from aqueous solution by wood, Process Saf. Environ. Protect. 76 (B2) (1998) 183–191.
[32] J.A. Dean, N.A. Lange, Handbook of Chemistry, McGraw-Hill, 1999.
[33] F.A. Cotton, G. Wilkinson, C.A. Murillo, M. Bochmann, Advanced Inorganic Chemistry, Wiley, Chichester, New York, 1999.
[34] J. Bajpai, R. Shrivastava, A.K. Bajpai, Dynamic and equilibrium studies on adsorption of Cr(VI) ions onto binary bio-polymeric beads of cross linked alginate and gelatin, Colloids Surf. A: Physicochem. Eng. Aspects 236 (1–3) (2004) 81–90.
[35] K.Y. Foo, B.H. Hameed, Insights into the modeling of adsorption isotherm systems, Chem. Eng. J. 156 (1) (2010) 2–10.
[36] I. Langmuir, The adsorption of gases on plane surfaces of glass, mica and platinum, J. Am. Chem. Soc. 40 (9) (1918) 1361–1403.
[37] H.M.F. Freundlich, Over the adsorption in solution, Zeitschrift Fur Physikalische Chemie-Stochiometrie Und Verwandtschaftslehre 57 (4) (1906) 385–470.
[38] R. Sips, On the structure of a catalyst surface, J. Chem. Phys. 16 (5) (1948) 490–495.
[39] Y. Liu, Is the free energy change of adsorption correctly calculated?, J Chem. Eng. Data 54 (7) (2009) 1981–1985.
[40] J. Kielland, Individual activity coefficients of ions in aqueous solutions, J. Am. Chem. Soc. 59 (9) (1937) 1675–1678.
[41] S.N.C. Ramos, A.L.P. Xavier, F.S. Teodoro, M.M.C. Elias, F.J. Gonçalves, L.F. Gil, R. P. Freitas, L.V.A. Gurgel, Modeling mono-and multi-component adsorption of cobalt (II), copper (II), and nickel (II) metal ions from aqueous solution onto a new carboxylated sugarcane bagasse. Part I: Batch adsorption study, Ind. Crops Prod. 74 (2015) 357–371.
[42] R.G. Pearson, Hard and Soft Acids and Bases, Dowden, Hutchinson & Ross, Stroudsburg, PA, USA, 1973.
[43] H. Irving, R.J.P. Williams, The stability of transition-metal complexes, J. Chem. Soc. (1953) 3192–3210.
[44] R. Schmuhl, H. Krieg, K. Keizer, Adsorption of Cu(II) and Cr(VI) ions by chitosan: kinetics and equilibrium studies, Water SA 27 (1) (2004) 1–8.
[45] G.Z. Kyzas, M. Kostoglou, N.K. Lazaridis, Copper and chromium(VI) removal by chitosan derivatives – Equilibrium and kinetic studies, Chem. Eng. J. 152 (2009) 440–448.
[46] Z. Yan, S. Haijia, T. Tianwei, Adsorption behaviors of the aminated chitosan adsorbent, Korean J. Chem. Eng. 24 (2007) 1047–1052.
[47] G.Z. Kyzas, M. Kostoglou, N.K. Lazaridis, D.N. Bikiaris, N-(2-Carboxybenzyl) grafted chitosan as adsorptive agent for simultaneous removal of positively and negatively charged toxic metal ions, J. Hazard. Mater. 244–245 (2013) 29–38.